

Security of round-robin differential-phase-shift quantum key distribution protocol with correlated light sources

Akihiro Mizutani¹ and Go Kato²

¹*Mitsubishi Electric Corporation, Information Technology R&D Center,
5-1-1 Ofuna, Kamakura-shi, Kanagawa, 247-8501 Japan*

²*NTT Communication Science Laboratories, NTT Corporation, 3-1,
Morinosato Wakamiya Atsugi-Shi, Kanagawa, 243-0198, Japan*

Among various quantum key distribution (QKD) protocols, the round-robin differential-phase-shift (RRDPS) protocol has a unique feature that its security is guaranteed without monitoring any statistics. Moreover, this protocol has a remarkable property of being robust against source imperfections assuming that the emitted pulses are independent. Unfortunately, some experiments confirmed the violation of the independence due to pulse correlations, and therefore the lack of a security proof without taking into account this effect is an obstacle for the security. In this paper, we prove that the RRDPS protocol is secure against any source imperfections by establishing a proof with the pulse correlations. Our proof is simple in the sense that we make only three experimentally simple assumptions for the source. Our numerical simulation based on the proof shows that the long-range pulse correlation does not cause a significant impact on the key rate, which reveals another striking feature of the RRDPS protocol. Our security proof is thus effective and applicable to wide range of practical sources and paves the way to realize truly secure QKD in high-speed systems.

I. INTRODUCTION

Quantum key distribution (QKD) offers information-theoretically secure communication between two distant parties, Alice and Bob [1]. To prove the security of QKD, we suppose mathematical models on the users' devices. If these models are discrepant from the physical properties of the actual devices, the security of actual QKD systems cannot be guaranteed. Hence, it is important to establish a security proof by reflecting the actual properties of the devices as accurately as possible.

One of the serious imperfections in the source device is the pulse correlation, which becomes a problem especially in high-speed QKD systems. Due to experimental imperfections, signal modulation for each emitted pulse affects the modulation of subsequent pulses. This means that information of Alice's setting choices, such as a bit choice and an intensity choice of the current pulse, is propagated to the subsequent pulses. Indeed, in [2], it is experimentally observed that the intensities are correlated among the adjacent pulses with GHz-clock QKD system. Even though tremendous efforts have been made so far to accommodate imperfections in the source into the security proofs (see e.g. [3]), such pulse correlation violates the assumption of most security proofs. The exceptions are the results in [2, 4, 5], where the intensity correlations between the nearest-neighbor pulses and arbitrary intensity correlations are respectively accommodated in [2] and [4], and the pulse correlation in terms of Alice's bit choice information is taken into account in [5]. Note that the result in [6] provides a security proof incorporating the correlation among the emitted pulses, but this correlation is assumed to be independent of Alice's setting choices.

Among various QKD protocols, the round-robin

differential-phase-shift (RRDPS) protocol [7] is one of the promising protocols, which has a unique feature that its security is guaranteed without monitoring any statistics such as the bit error rate. Thanks to this property, the RRDPS protocol has a better tolerance on the bit error rate than the other protocols and the fast convergence in the finite key regime. For this protocol, a number of works have been done theoretically [8–16] and experimentally [17–21]. Moreover, the RRDPS protocol is shown to be robust against most of source imperfections [8], which is a remarkable property. However, this robustness is maintained only when the pulses emitted from the source are independent, which is also assumed in all the previous security proofs of the RRDPS protocol [9–16]. Unfortunately, some experiment [2] confirms the violation of this independence due to the pulse correlations, and hence the lack of a security proof without taking into account this effect is an obstacle for guaranteeing the implementation security of the RRDPS protocol.

In this paper, we show that the RRDPS protocol is secure against any source imperfections by establishing the security proof with the pulse correlations. We adopt a general correlation model in which a bit information Alice selected is encoded not only on the current pulse but also on the subsequent pulses. In our security proof, we make only three experimentally simple source assumptions, which would be useful for simple source characterization. More specifically, we assume the length of the correlation among the emitted pulses, the fidelity between two emitted states when the correlation patterns are different, and the lower bounds on the vacuum emission probabilities of each emitted pulse. It is remarkable that no other detailed characterization is required for the source and any side-channels in the source can be accommodated. In the security proof, we exploit the

reference technique [5] that is a general framework of a security proof to deal with source imperfections, including the pulse correlation. As a result of our security proof, we show that the long-range pulse correlation does not cause a significant impact on the key rate under a realistic experimental setting, which reveals another striking property of the RRDPS protocol.

II. RESULTS

A. Notations

Throughout the paper, we adopt the following notations. Let N be the total number of pulses sent by Alice in the protocol. For any symbol A , we define $A_i := A_i, A_{i-1}, \dots, A_1$ with $i \in \mathbb{N}$ and $A_{\geq i} := A_N, A_{N-1}, \dots, A_i$. We denote by $\{|0\rangle, |1\rangle\}$ the Z -basis eigenstates in the qubit space, and let $|\pm\rangle := (|0\rangle \pm |1\rangle)/\sqrt{2}$ be the X -basis eigenstates. For any bit sequence κ , $|\kappa|$ denotes the length of the bit sequence κ .

B. The idea to apply reference technique to RRDPS protocol

Here, we explain how to apply the reference technique (RT) [5] to deal with the pulse correlations in the RRDPS protocol. In the original RRDPS protocol [7], Alice sends a block of pulses from which Alice and Bob try to extract one-bit key using a variable-delay interferometer. On the other hand, in our protocol with the correlation length of l_c , Alice and Bob divide each emitted block into $(l_c + 1)$ groups and try to extract $(l_c + 1)$ -bit key from each of the groups. In so doing, Bob employs $(l_c + 1)$ variable-delay interferometers so that the pulses belonging to the same group interfere. In other terms, our protocol can be regarded as running $(l_c + 1)$ RRDPS protocols simultaneously. We adopt such a modification for enabling us to apply the RT. Below, we explain why the modification is needed.

In the RT, we consider an entanglement-based picture where each k^{th} emitted pulse is entangled with the qubit. To discuss the security of the k^{th} bit j_k that is obtained by measuring the qubit in the Z -basis, each qubit is measured in the X -basis. Since how well Alice can predict the X -basis measurement outcome is directly related to the amount of privacy amplification [22], this estimation is crucial in proving the security. The RT provides a method for its estimation under the pulse correlation, but one vital point is that the set of the k^{th} emitted states must be fixed just before the emission of the k^{th} pulse. To fix the set, we consider to measure the previous l_c qubits in the Z -basis. For instance, if $l_c = 1$, to discuss the security of the even-indexed bit j_{2k} , the previous odd-indexed qubit must be measured in the Z -basis. These

Z -basis measurements of the previous l_c qubits conflict the original security proof [7] of the RRDPS protocol. This is because to estimate the aforementioned X -basis statistics, all the qubits in the block are measured in the X -basis since any two pulses in the block can interfere in Bob's measurement. To avoid this conflict, for instance if $l_c = 1$, we modify the RRDPS protocol such that the even-indexed and the odd-indexed pulses interfere separately, and the secret keys are separately extracted from each interference using two interferometers. In doing so, when we discuss the security of the even-indexed bit, only the even-indexed qubits in the block are measured in the X -basis while the odd-indexed ones are measured in the Z -basis. Hence, thanks to this modification, we can realize both the X - and the Z -basis measurements at the same time. By generalizing this idea to any $l_c \geq 2$, if we use $(l_c + 1)$ interferometers and consider the protocol that extracts the keys from each interferometer, these two basis measurements become compatible, and hence we can apply the RT for proving the security.

We remark that when $l_c = 1$, the security proofs for the even- and the odd-indexed keys are mutually exclusive in the sense that the proof for the odd-indexed (even-indexed) key provides us with how much privacy amplification needs to be applied to the odd-indexed (even-indexed) key, but it does not offer the security of the even-indexed (odd-indexed) key. Fortunately, thanks to the universal composability [23] of the two security proofs, the amount of privacy amplification to generate the key both from the odd- and the even-indexed bits simultaneously is equivalent to those obtained from the mutually exclusive proofs. This argument holds for any $l_c \geq 2$ due to the universal composability of the $(l_c + 1)$ security proofs.

C. Assumptions on the devices

Before describing the protocol, we summarize the assumptions we make on the source and the receiver. Figure 1 depicts the setups of Alice and Bob's devices employed in the protocol. First, we list up the assumptions on Alice's source as follows. As long as the following assumptions hold, any side-channel in the source can be accommodated.

(A1) For each k^{th} emitted pulse ($1 \leq k \leq N$), Alice chooses a random bit $j_k \in \{0, 1\}$. The bit j_k is encoded not only to the k^{th} emitted pulse but also to the subsequence pulses. Let $l_c \geq 0$ be the number of pulses that the information j_k is propagated, and we call l_c correlation length. Let $|\psi_{j_k|j_{k-1}, \dots, j_1}\rangle_{B_k} = |\psi_{j_k|j_{k-1}}\rangle_{B_k}$ be the state of the k^{th} emitted signal to Bob, where the subscripts j_{k-1}, \dots, j_1 indicate the dependency of the previous information j_{k-1}, \dots, j_1 . Note that j_0 represents

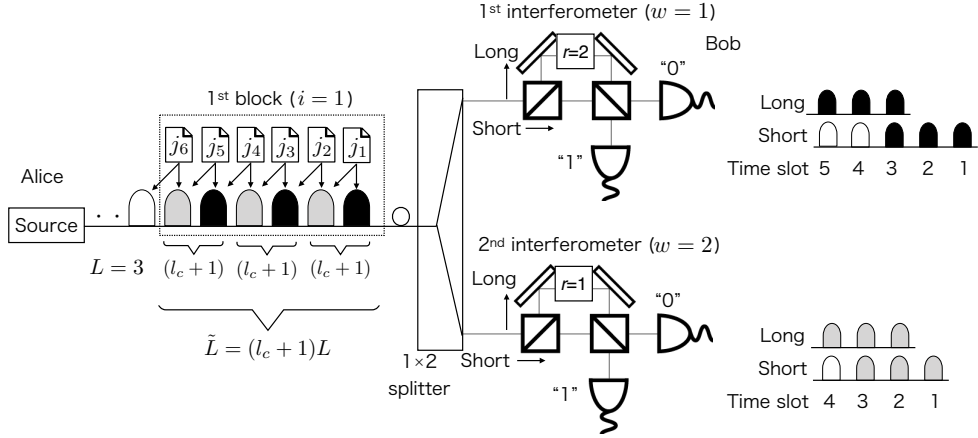


FIG. 1: The setups of the source and the measurement devices under nearest neighbor correlation ($l_c = 1$), the number of pulses in each of the block to be fed into each of the interferometer L being three ($L = 3$), and block size being 6 ($\tilde{L} = (l_c + 1)L = 6$). For the 1st block ($i = 1$), the positions of the black [gray] pulses belong to the 1st group ($w = 1$), that is, $\mathcal{G}_{w=1}^{(1)} = \{1, 3, 5\}$ [2nd group ($w = 2$), that is, $\mathcal{G}_{w=2}^{(1)} = \{2, 4, 6\}$]. The black and gray pulses are respectively corresponds to $w = 1$ and $w = 2$, which are fed to the 1st and the 2nd variable-delay interferometer with two 50:50 beam splitters, respectively. Here, the delay r is randomly chosen from the set $\{1, 2\}$. The pulse trains from the interferometer are measured by two photon-number-resolving detectors representing bit values “0” and “1”. The successful detection in each of the interferometers occurs if Bob detects a single-photon in total among the $(r + 1)^{\text{th}}$ to the L^{th} time slots.

having no condition. In this paper, we consider the case where Alice employs \tilde{L} pulses contained in a single-block, where \tilde{L} is set to be $(l_c + 1)L$ for $L \geq 3$. We call \tilde{L} pulses of systems $B_{(i-1)\tilde{L}+1}, \dots, B_{i\tilde{L}}$ the i^{th} block.

(A2) When $l_c \geq 1$, for any k ($1 \leq k \leq N$) and any ζ ($k + 1 \leq \zeta \leq k + l_c$), the following parameter $\epsilon_{\zeta-k} \geq 0$ characterizing the correlation is available.

$$\begin{aligned} & \left| \langle \psi_{j_\zeta | j_{\zeta-1}, \dots, j_{k+1}, j_k = 1, j_{k-1}} | \psi_{j_\zeta | j_{\zeta-1}, \dots, j_{k+1}, j_k = 0, j_{k-1}} \rangle \right|^2 \\ & \geq 1 - \epsilon_{\zeta-k}. \end{aligned} \quad (1)$$

Note that the difference between both states in the inner product is in the j_k^{th} index. The parameter $\epsilon_{\zeta-k}$ depends only on the difference $\zeta - k$, but it is independent of $j_\zeta, j_{\zeta-1}, \dots, j_{k+1}, j_{k-1}, \dots, j_1$. Note that by the assumption (A1), if $\zeta \geq k + l_c + 1$, the left hand size of Eq. (1) is equal to 1 since the bit information j_k does not propagate to the ζ^{th} state.

(A3) For any k ($1 \leq k \leq N$) and any $j_k \in \{0, 1\}$, the vacuum emission probability of state $|\psi_{j_k | j_{k-1}, \dots, j_1}\rangle$ is lower-bounded by $p_{\text{vac}, j_k}^{\text{L}}$ regardless of k and the previous choices of j_{k-1}, \dots, j_1 . Mathematically, we suppose that

$$\text{tr} [|\text{vac}\rangle \langle \text{vac} | \psi_{j_k | j_{k-1}} \rangle \langle \psi_{j_k | j_{k-1}} |] \geq p_{\text{vac}, j_k}^{\text{L}}, \quad (2)$$

where $|\text{vac}\rangle$ denotes the vacuum state.

Providing the method for experimentally measuring the bounds in Eqs. (1) and (2) is beyond the scope of this paper. Note that the assumption (A2) can be alternatively

expressed by using $p_{\text{vac}, 0}^{\text{L}}$ and $p_{\text{vac}, 1}^{\text{L}}$ in Eq. (2) because as we will show in Appendix A, the inner product in Eq. (1) can be lower-bounded as

$$\begin{aligned} & \left| \langle \psi_{j_\zeta | j_{\zeta-1}, \dots, j_{k+1}, j_k = 1, j_{k-1}} | \psi_{j_\zeta | j_{\zeta-1}, \dots, j_{k+1}, j_k = 0, j_{k-1}} \rangle \right| \\ & \geq \begin{cases} 2p_{\text{vac}, j_\zeta}^{\text{L}} - 1 & \text{if } 2p_{\text{vac}, j_\zeta}^{\text{L}} \geq 1 \\ 0 & \text{otherwise.} \end{cases} \end{aligned} \quad (3)$$

Next, we list up the assumptions on Bob's measurement. In this paper, we consider that Alice and Bob try to extract $(l_c + 1)$ secret keys i.e., they divide each block into $(l_c + 1)$ groups and try to generate a one bit key from each of the groups. In so doing, Bob employs $(l_c + 1)$ variable-delay interferometers with $(L - 1)$ delays followed by two detectors¹. To explain this more clearly, we classify the set $\{(i-1)\tilde{L}+1, (i-1)\tilde{L}+2, \dots, i\tilde{L}\}$ of the positions of the emitted pulses associated with the i^{th} block into $(l_c + 1)$ groups, and the w^{th} group ($w \in \{1, 2, \dots, l_c + 1\}$) for the i^{th} block is defined by

$$\mathcal{G}_w^{(i)} := \{(l_c + 1)(m - 1) + w + (i - 1)\tilde{L}\}_{m=1}^L. \quad (4)$$

Note that w^{th} group $\mathcal{G}_w^{(i)}$ is constructed by picking up all the k^{th} pulses from the i^{th} block with $k \equiv w$ in modulo $(l_c + 1)$. For instance, if $i = 1, l_c = 2, L = 10$ and $\tilde{L} = 30$, $\mathcal{G}_{w=1}^{(1)} = \{1, 4, 7, \dots, 28\}, \mathcal{G}_{w=2}^{(1)} = \{2, 5, 8, \dots, 29\}$

¹ Note that each interferometer followed by two detectors considered in this paper is the same configuration as the one in the original RRDPS protocol [7].

and $\mathcal{G}_{w=3}^{(1)} = \{3, 6, 9, \dots, 30\}$. Then, Bob prepares $(l_c + 1)$ interferometers, and for each i^{th} block, he feeds the incoming pulses of systems $\{B_k\}_{k \in \mathcal{G}_w^{(i)}}$ to the w^{th} interferometer.

- (B1) Bob uses an optical splitter with one-input and $(l_c + 1)$ -output to feed the pulses in the i^{th} block into the $(l_c + 1)$ interferometers. The role of the splitter is regarded as routing the pulses to an appropriate interferometer, where the k^{th} pulse with $k \in \mathcal{G}_w^{(i)}$ is fed to the w^{th} interferometer.
- (B2) Followed by the optical splitter, Bob employs the $(l_c + 1)$ variable-delay interferometers with two 50:50 beam splitters (BSs), where the delay of the interferometer is chosen uniformly at random from a set $\{1, 2, \dots, L - 1\}$. When r -bit delay ($r \in \{1, 2, \dots, L - 1\}$) is chosen in the interferometer, two pulses that are $r(l_c + 1)$ -pulses apart in terms of the pulses Alice emitted interfere.
- (B3) After the interferometer, the pulses are detected at time slots 1 through $L + r$ by two photon-number-resolving (PNR) detectors, which discriminates the vacuum, a single-photon, and two or more photons of a specific optical mode. Each of the detectors is associated to bit values 0 and 1, respectively. We suppose that the quantum efficiencies and dark countings are the same for both detectors.
- (B4) We suppose that there are no side-channels in Bob's measurement device.

D. Protocol

In this section, we describe the actual protocol of the RRDPS protocol under the pulse correlations in the source device. Let N_{em} be the number of emitted blocks sent by Alice, and the total number of pulses sent by Alice is $N = N_{\text{em}}\tilde{L}$. As we will see below, our protocol can be regarded as running $(l_c + 1)$ RRDPS protocols simultaneously, each of which employs a block containing \tilde{L} pulses. More specifically, our protocol runs as follows.

1. Alice and Bob respectively repeat steps 2 and 3 for $i = 1, \dots, N_{\text{em}}$.
2. Alice chooses a sequence of random bits $j_{(i-1)\tilde{L}+1}, \dots, j_{i\tilde{L}} \in \{0, 1\}^{\tilde{L}}$, and sends Bob the pulses in the following state through the quantum channel:

$$\bigotimes_{k=(i-1)\tilde{L}+1}^{i\tilde{L}} |\psi_{j_k|j_{k-1}, \dots, j_1}\rangle_{B_k}. \quad (5)$$

3. By the optical splitter with one-input and $(l_c + 1)$ -output, the pulses in the i^{th} block are split to feed into the $(l_c + 1)$ variable-delay interferometers. Among the pulses in the i^{th} block, the k^{th} pulse with $k \in \mathcal{G}_w^{(i)}$ is fed to the w^{th} interferometer.

Bob executes the following for $w = 1, \dots, l_c + 1$. At the w^{th} interferometer, Bob randomly selects the delay $r \in \{1, 2, \dots, L - 1\}$, splits L incoming pulses into two trains of pulses using a 50:50 BS, and shifts backwards only one of the two trains by r . Recall that the time of a single shift is equal to $(l_c + 1)$ -times as long as the interval of the neighboring emitted pulses. Then, Bob lets each of the first $L - r$ pulses in the shifted train interfere with each of the last $L - r$ pulses in the other train with the other 50:50 BS, and detects photons with the two PNR detectors at time slots 1 through $L + r$.

- (a) When Bob detects exactly one photon among the $(r + 1)^{\text{th}}$ to the L^{th} time slots and observes no detection at the other time slots, he records a sifted key bit $z_{B,i}^{(w)} \in \{0, 1\}$ depending on which detector reported the single photon. He also records the unordered pair $\{u_i^{(w)}, v_i^{(w)}\}$, which are the positions of the pulse pair that resulted in the successful detection ($u_i^{(w)}, v_i^{(w)} \in \{1, 2, \dots, L\}, |u_i^{(w)} - v_i^{(w)}| = r$). He announces "success" and $\{u_i^{(w)}, v_i^{(w)}\}$ over the classical channel.
- (b) In all the cases other than (a), Bob announces "failure" and w through the classical channel.
- 4. Bob executes the following for $w = 1, \dots, l_c + 1$. Let $N_{\text{suc}}^{(w)}$ be the number of success blocks observed at the w^{th} interferometer. For these blocks, Bob defines his w^{th} type sifted key $\mathbf{z}_B^{(w)}$ by concatenating his sifted key bits $z_{B,i}^{(w)}$ for $i \in \mathcal{B}_{\text{suc}}^{(w)}$. Here, the set $\mathcal{B}_{\text{suc}}^{(w)}$ is composed of the block-index i where the pulses whose indices in the set $\mathcal{G}_w^{(i)}$ result in the successful detection.
- 5. Alice executes the following for $w = 1, \dots, l_c + 1$. Alice calculates her sifted key bit $z_{A,i}^{(w)} = j_{k_1} \oplus j_{k_2}$ for $i \in \mathcal{B}_{\text{suc}}^{(w)}$ with k_1 and k_2 being the $u_i^{(w)}$ -th and the $v_i^{(w)}$ -th elements of $\mathcal{G}_w^{(i)}$, and defines her w^{th} type sifted key $\mathbf{z}_A^{(w)}$ by concatenating her raw key bits $z_{A,i}^{(w)}$ for $i \in \mathcal{B}_{\text{suc}}^{(w)}$.
- 6. Bob corrects the bit errors in $\mathbf{z}_B := (\mathbf{z}_B^{(1)}, \dots, \mathbf{z}_B^{(l_c+1)})$ to make it coincide with $\mathbf{z}_A := (\mathbf{z}_A^{(1)}, \dots, \mathbf{z}_A^{(l_c+1)})$ by sacrificing $|\mathbf{z}_A|f_{\text{EC}}$ bits of encrypted public communication from Alice

by consuming the same length of a pre-shared secret key.

7. Alice and Bob executes the following for $w = 1, \dots, l_c + 1$.

For each w^{th} type reconciled key, Alice and Bob conduct privacy amplification by shortening their keys by $|\mathbf{z}_A^{(w)}|f_{\text{PA}}^{(w)}$ to obtain the final keys.

In this paper, we only consider the secret key rate in the asymptotic limit of an infinite sifted key length. We consider the asymptotic limit of large N_{em} while the following observed parameters are fixed:

$$0 \leq Q^{(w)} := \frac{N_{\text{suc}}^{(w)}}{N_{\text{em}}} \leq 1. \quad (6)$$

Note that f_{EC} in step 6 is determined as a function of the bit error rate e_{bit} in \mathbf{z}_A and \mathbf{z}_B , where e_{bit} can be estimated by random sampling whose cost is negligible in the asymptotic limit. Also, the fraction of privacy amplification $f_{\text{PA}}^{(w)}$ in step 7 is determined by the experimentally available observables $Q^{(w)}$ in Eq. (6), $\{\epsilon_d\}_{d=1}^{l_c}$ in Eq. (1), $p_{\text{vac},0}^{\text{L}}$ and $p_{\text{vac},1}^{\text{L}}$ in Eq. (2), whose explicit form is given the next section.

E. Security proof

Here, we summarize the result of the security proof of the protocol described above and determine the amount of privacy amplification $|\mathbf{z}_A^{(w)}|f_{\text{PA}}^{(w)}$ for the w^{th} type sifted key in the asymptotic limit. As will be explained in this section, our security proof is based on the complementarity scenario [22] in which estimation of an upper bound on the phase error rate assures the security. The main result is this upper bound, which is given in Theorem 1, and we provide its derivation in Methods section. Here, we outline the crux of the discussions. The difficulty of our phase error rate estimation comes from the correlations among the emitted pulses that have not been accommodated in the previous security proofs of the RRDPS protocol [8–16]. We solve this problem by exploiting the *reference technique* established in [5]. This is a technique that simplifies the estimation of the phase error rate when the actually employed states are close to the ones whose formula associated to the phase error rate is easily derived. In this technique, we consider reference states, which are fictitious states that are not prepared in the protocol but close to the actual state. The key intuition is rather simple; when the reference states and the actual states are close, the deviation between probabilities associated to the reference states and those associated to the actual states should not be large. Therefore, we can obtain the phase error rate formula for the actual states by slightly modifying the formula for the reference states. We emphasize that Alice does not need to

generate the reference states in the protocol, and they are purely a mathematical tool for phase error rate estimation. In particular, we choose the reference states regarding the k^{th} emitted pulse such that the information j_k is *only* encoded to system B_k (see Eq. (26) for the explicit formula). By exploiting this property, it is simple to obtain the probabilities for the reference states, which will be given by T in Eq. (21). Depending on the fidelity between the actual and reference states, which will be given by S in Eq. (22), by slightly modifying the relationship for the reference states, we finally obtain the target probability with the actual ones.

In the rest of this section, we first explain the structure of the security proof, define the parameters that are needed to present the main result, and then describe Theorem 1. For the security proof with complementarity, we consider alternative entanglement-based procedures for Alice's state preparation at step 2 and calculation of her raw key bit $z_{A,i}^{(w)}$ at step 5. These alternative procedures can be employed to prove the security of the actual protocol because the states sent to an eavesdropper (Eve), Bob's measurement, and the final key are identical to those in the actual protocol. Also, Bob's public announcement of the unordered pair $\{u_i^{(w)}, v_i^{(w)}\}$ in the actual protocol is identical to the one in the alternative protocol. As for Alice's state preparation at step 2, she alternatively prepares N auxiliary qubits in systems \mathbf{A}_N , which remain at Alice's laboratory during the whole protocol, and the N pulses in systems \mathbf{B}_N to be sent, in the following state

$$|\Psi\rangle_{\mathbf{A}_N \mathbf{B}_N} := \frac{1}{\sqrt{2^N}} \sum_{j_N=0}^1 \cdots \sum_{j_1=0}^1 \bigotimes_{k=1}^N |j_k\rangle_{A_k} |\psi_{j_k|j_{k-1}}\rangle_{B_k}. \quad (7)$$

We note that from Eve's perspective, the states of system B_k in Eqs. (5) and (7) are equivalent. As for calculation of the sifted key bit $z_{A,i}^{(w)} = j_{k_1} \oplus j_{k_2}$ at step 5, this bit can be alternatively extracted by applying the controlled-not gate (defined on the Z -basis) on the k_1^{th} and k_2^{th} auxiliary qubits of systems A_{k_1} and A_{k_2} with the k_1^{th} one being the control and the k_2^{th} one being the target followed by measuring the k_2^{th} auxiliary qubit in the Z -basis to obtain $z_{A,i}^{(w)}$.

In the complementarity scenario, the discussion of the security of the key $\mathbf{z}_A^{(w)}$ is equivalent to consider a virtual scenario of how well Alice can predict the outcome of the measurement complementary to the one to obtain $z_{A,i}^{(w)}$. In particular, we take the X -basis measurement as the complementary basis, and we need to quantify how well Alice can predict its outcome $x_{k_2} \in \{+, -\}$ on system A_{k_2} . As for Bob, instead of aiming at learning $z_{A,i}^{(w)}$, he performs the alternative measurement that determines which of the k^{th} pulse in the group $\mathcal{G}_w^{(i)}$ contains the single-photon. This measurement is a complementary

to the one for obtaining his sifted key bit $z_{B,i}^{(w)}$. With this alternative measurement, Bob announces the pair $\{u_i^{(w)}, v_i^{(w)}\}$ such that the first index $u_i^{(w)}$ corresponds to the location of the single-photon and the second index $v_i^{(w)}$ is chosen uniformly at random from the set $\{1, 2, \dots, i-1, i+1, i+2, \dots, L\}$. Hence, in this virtual scenario, Alice's task is to predict the outcome x_{k_2} where k_2 is chosen uniformly at random from the group $\mathcal{G}_w^{(i)}$ except for k_1 . We define the occurrence of *phase error* to be the case where Alice fails in her prediction of the outcome x_{k_2} . Let $N_{\text{ph}}^{(w)}$ denote the number of phase errors of the w^{th} type sifted key among $|z_A^{(w)}|$ trials. Suppose that the upper bound $N_{\text{ph}}^{(w),\text{U}}$ on $N_{\text{ph}}^{(w)}$ is obtained as a function of the experimentally available observables $Q^{(w)}$ in Eq. (6), $\{\epsilon_d\}_{d=1}^{l_c}$ in Eq. (1), $p_{\text{vac},0}^{\text{L}}$ and $p_{\text{vac},1}^{\text{L}}$ in Eq. (2). In this case, in the asymptotic limit, a sufficient fraction of privacy amplification is given by [22]

$$f_{\text{PA}}^{(w)} = h\left(N_{\text{ph}}^{(w),\text{U}}/N_{\text{suc}}^{(w)}\right), \quad (8)$$

where $h(x)$ is defined by $h(x) = -x \log_2 x - (1-x) \log_2(1-x)$ for $0 \leq x \leq 0.5$ and $h(x) = 1$ for $x > 0.5$. Our main result, Theorem 1, derives the upper bound $e_{\text{ph}}^{(w),\text{U}}$ on the phase error rate $e_{\text{ph}}^{(w)} := N_{\text{ph}}^{(w)}/N_{\text{suc}}^{(w)}$ with $Q^{(w)}$, $\{\epsilon_d\}_{d=1}^{l_c}$, $p_{\text{vac},0}^{\text{L}}$ and $p_{\text{vac},1}^{\text{L}}$ (see Methods section for the proof).

Theorem 1 *In the asymptotic limit of large key length of the w^{th} type sifted key $|z_A^{(w)}|$, the upper bound on the phase error rate for the w^{th} type sifted key of the RRDPS protocol is given by*

$$e_{\text{ph}}^{(w),\text{U}} = \sum_{s=0}^{L-2} \frac{1}{L-1} \min\left\{\frac{\nu(L, s, C)}{Q^{(w)}}, 1\right\}. \quad (9)$$

Here, function $\nu(L, s, C)$ is defined by

$$\nu(L, s, C) := \sum_{y=s+1}^L \binom{L}{y} C^y (1-C)^{L-y},$$

where $C = g(T, S)$ if $T \leq S^2$ and $C = 1$ otherwise with $T := 1 - \left(\sqrt{p_{\text{vac},0}^{\text{L}}} + \sqrt{p_{\text{vac},1}^{\text{L}}}\right)^2/4$, $S := (1 + \prod_{d=1}^{l_c} \sqrt{1-\epsilon_d})/2$ for $l_c \geq 1$ and $S=1$ for $l_c = 0$, and $g(x, y) := x + (1-y^2)(1-2x) + 2y\sqrt{(1-y^2)x(1-x)}$.

We remark that once characterizations of the source device are completed (i.e., $\{\epsilon_d\}_{d=1}^{l_c}$, $p_{\text{vac},0}^{\text{L}}$ and $p_{\text{vac},1}^{\text{L}}$ are obtained), C becomes a constant. Theorem 1 reveals that as the correlation length l_c gets larger, $\nu(L, s, C)$ in the expression of the phase error rate in Eq. (9) generally gets larger because $C = g(T, S)$ is a monotonically decreasing function of S and S generally gets smaller as l_c becomes larger.

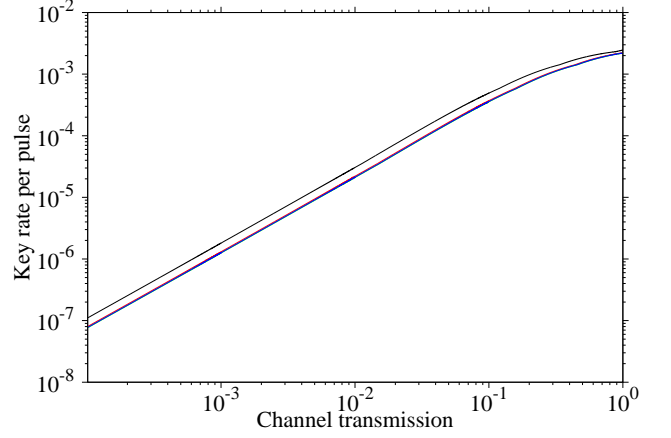


FIG. 2: Secure key rate R per pulse as a function of the overall channel transmission η . From top to bottom, we plot the key rates for $(l_c, \Delta) = (0,0), (1,0.2), (2,0.2)$ and $(10,0.2)$ with $e_{\text{bit}} = 3\%$ and $L = 32$. We note that the key rates for the last three parameters are almost superposed.

Finally, using Theorem 1, the secret key rate per pulse is given by

$$R = \sum_{w=1}^{l_c+1} Q^{(w)} \left[1 - f_{\text{EC}} - h\left(e_{\text{ph}}^{(w),\text{U}}\right) \right] / (l_c + 1)L. \quad (10)$$

F. Simulation of secure key rates

Here, we show the simulation results of asymptotic key rate R per pulse given by Eq. (10) as a function of the overall channel transmission η including the detector efficiency. For the simulation, we assume that each emitted pulse is a coherent pulse from a conventional laser with mean photon number μ and only the phases of the coherent pulses are correlated. In this case, the lower bound on the vacuum emission probability $p_{\text{vac},j_k}^{\text{L}}$ in Eq. (2) is given by $e^{-\mu}$ and hence T defined above is $1 - e^{-\mu}$. For the simulation, we consider the cases of the correlation length $l_c = 0, 1, 2$ and 10 , and for all the cases, we adopt $f_{\text{EC}} = h(e_{\text{bit}})$ with e_{bit} denoting the bit error rate in the protocol and suppose the successful detection rate for any w as $Q^{(w)} = L\eta\mu e^{-L\eta\mu}/2$.

In the case of $l_c = 1$, namely, the case of the nearest neighbor correlation, we assume that the k^{th} emitted state is written as

$$|\psi_{j_k|j_{k-1}}\rangle = \delta_{j_{k-1},0}|(-1)^{j_k}\sqrt{\mu}\rangle + \delta_{j_{k-1},1}|(-1)^{j_k}\sqrt{\mu}e^{i\Delta}\rangle. \quad (11)$$

Here, $\delta_{x,y}$ is the Kronecker delta and $|e^{i\theta}\sqrt{\mu}\rangle$ denotes the coherent state with the complex amplitude being $e^{i\theta}\sqrt{\mu}$. This state represents the pulse correlation that if the previous choice of bit j_{k-1} is 0, then the next k^{th} states are the ideal states $\{|\sqrt{\mu}\rangle, |-\sqrt{\mu}\rangle\}$, but if j_{k-1} is 1, then the

phases are deviated by Δ from the ideal ones. In this setting, S defined above is given by

$$S = \frac{1 + \sqrt{1 - \epsilon_1}}{2} = \frac{1 + |\langle \sqrt{\mu} | \sqrt{\mu} e^{i\Delta} \rangle|}{2} = \frac{1 + e^{\mu(\cos \Delta - 1)}}{2}.$$

In the case of $l_c = 2$, we assume that the k^{th} emitted state is written as $|\psi_{j_k|j_{k-1},j_{k-2}}\rangle = \delta_{j_{k-1},0}\delta_{j_{k-2},0}|(-1)^{j_k}\sqrt{\mu}\rangle + \delta_{j_{k-1},0}\delta_{j_{k-2},1}|(-1)^{j_k}\sqrt{\mu}e^{i\Delta/2}\rangle + \delta_{j_{k-1},1}\delta_{j_{k-2},0}|(-1)^{j_k}\sqrt{\mu}e^{i\Delta}\rangle + \delta_{j_{k-1},1}\delta_{j_{k-2},1}|(-1)^{j_k}\sqrt{\mu}e^{i3\Delta/2}\rangle$. This state represents that if $j_{k-1} = 1$ ($j_{k-2} = 1$), the phases of the k^{th} pulses are rotated by Δ ($\Delta/2$). This means that the influence of second-previous bit j_{k-2} to the k^{th} pulse is half of that of the previous bit j_{k-1} . In this setting, S is given by

$$S = \frac{1 + \sqrt{1 - \epsilon_1}\sqrt{1 - \epsilon_2}}{2} = \frac{1 + e^{\mu(\cos \Delta - 1)}e^{\mu(\cos \frac{\Delta}{2} - 1)}}{2}.$$

As for the case of $l_c = 10$, the k^{th} state is set to be analogous to the one for $l_c = 1, 2$ where if $j_{k-d} = 1$ (with $d = 1, \dots, 10$), the phases of the k^{th} pulses are rotated by $\Delta/2^{d-1}$. A direct calculation shows $S = (1 + \prod_{d=1}^{10} \sqrt{1 - \epsilon_d})/2 = (1 + \prod_{d=1}^{10} e^{\mu(\cos(\Delta/2^{d-1}) - 1)})/2$.

In Fig. 2, we plot the key rates for $e_{\text{bit}} = 0.03$, $L = 32$ and $\Delta = 0.2$ rad for the cases of $l_c = 0, 1, 2, 10$ from top to bottom. The top line is the key rate with no pulse correlation (i.e., $l_c = 0$) that corresponds to $\Delta = 0$ in Eq. (11). The key rates are optimized over mean photon number μ for each value of channel transmission η . From these lines, we see that the pulse correlation slightly degrades the key rate (about 0.7 times lower than the one without pulse correlation), but the three lines with $l_c = 1, 2$ and 10 are almost superposed. This implies that when the pulse correlation gets weaker as the pulses are farther apart, which is assumed in our simulation, the long-range pulse correlation does not cause a significant impact on the key rate.

III. DISCUSSION

In this paper, we have provided the information theoretic security proof of the RRDPS protocol with the pulse correlation in Alice's source by using the reference technique. The pulse correlation is one of the serious imperfections in high-speed QKD systems where Alice's random bit choice is propagated to the subsequent emitted pulses. Once the number of propagated pulses (l_c) is fixed, our security proof only requires the two experimentally simple assumptions on the source: the lower bound on the fidelity between the two k^{th} states when the correlation patterns are different and the lower bounds on the vacuum emission probabilities of each emitted pulse.

Our numerical simulations have shown the key rates up to $l_c = 10$ and have revealed that the long-range pulse correlation does not cause a significant impact on the key rate in a realistic experimental setting. Therefore, our security proof is effective and applicable to wide range of practical sources, and thus paves the way to realize the truly secure and high-speed QKD systems.

We end with some open questions. It has an practical importance to simulate the key rates based on another source correlation model such as an intensity correlation that is beyond the one we have supposed in our simulation shown in Fig. 2. Also, it is interesting to extend our security proof to accommodate quantum correlations among the emitted pulses.

IV. METHODS

In this section, we prove our main result, Theorem 1.

A. Derivation of the phase error rate for the w^{th} type sifted key

Here, we derive the upper bound $e_{\text{ph}}^{(w),\text{U}}$ on the phase error rate $e_{\text{ph}}^{(w)} := N_{\text{ph}}^{(w)}/N_{\text{suc}}^{(w)}$ for the w^{th} type sifted key ($w \in \{1, 2, \dots, l_c + 1\}$). We remark that the following discussions hold for any w . To derive $e_{\text{ph}}^{(w),\text{U}}$, we consider performing the X -basis measurement on system A_k of $|\Psi\rangle_{A_N B_N}$ in Eq. (7) with k belonging to the w^{th} group of indices $\bigcup_{i=1}^{N_{\text{em}}} \mathcal{G}_w^{(i)}$. We then evaluate the upper bound on the probability of obtaining the outcome of the minus when system A of the m^{th} element ($1 \leq m \leq L$) of set $\mathcal{G}_w^{(i)}$ is measured in the X -basis. Mathematically, the target for computation is the probability $\Pr[x_t = -|\{x_k\}_{k \in \mathcal{P}_{i,m}}]$ with

$$t := (i-1)\tilde{L} + w + (m-1)(l_c + 1),$$

$$\mathcal{P}_{i,m} := \bigcup_{a=1}^i \{k | k \in \mathcal{G}_w^{(a)}, k < t\}.$$

If $\Pr[x_t = -|\{x_k\}_{k \in \mathcal{P}_{i,m}}, j_{t-1}, \dots, j_{t-l_c}] \leq C$ with constant C holds for any $j_{t-1}, \dots, j_{t-l_c} \in \{0, 1\}^{l_c}$, where $j_k \in \{0, 1\}$ denotes the Z -basis measurement outcome on system A_k of Eq. (7), applying the Bayes rule leads that the target probability is also upper-bounded by C :

$$\Pr[x_t = -|\{x_k\}_{k \in \mathcal{P}_{i,m}}] \leq C. \quad (12)$$

The derivation of the upper-bound C involves the reference technique established in [5], and we explain its detail in the next section.

With Eq. (12) in hand, by considering the binomial trial with success probability C , the total number of the minus $n_{w,-}^{(i)}$ obtained through measuring L

systems $\{A_k\}_{k \in \mathcal{G}_w^{(i)}}$ obeys the following probability distribution when conditioned on the previous outcomes $n_{w,-}^{(i-1)}, \dots, n_{w,-}^{(1)}$:

$$\Pr[n_{w,-}^{(i)} > s | n_{w,-}^{(i-1)}, \dots, n_{w,-}^{(1)}] \leq \sum_{y=s+1}^L \binom{L}{y} C^y (1-C)^{L-y} =: \nu(L, s, C). \quad (13)$$

Here, s denotes the integer. Once s is fixed, $\nu(L, s, C)$ is constant independently of the block index i ($1 \leq i \leq N_{\text{em}}$).

Finally, we derive the upper bound $e_{\text{ph}}^{(w), \text{U}}$. For this, we classify $N_{\text{suc}}^{(w)}$ successfully detected blocks according to $n_{w,-}$, which leads to $N_{\text{ph}}^{(w)} = \sum_{s=0}^L N_{\text{ph}|n_{w,-}=s}^{(w)}$. By considering Bob's alternative measurement explained in Sec. II E, the probability of failing in the prediction of the X -basis measurement outcome (namely, having the occurrence of the phase error) when $n_{w,-} = s$ is $s/(L-1)$. Hence, the Chernoff bound leads the following for any $\zeta > 0$

$$\begin{aligned} e_{\text{ph}}^{(w)} &\leq \sum_{s=0}^{L-1} \frac{s}{L-1} \frac{N_{\text{suc}, n_{w,-}=s}^{(w)}}{N_{\text{suc}}^{(w)}} + \zeta + \frac{N_{\text{suc}, n_{w,-}=L}^{(w)}}{N_{\text{suc}}^{(w)}} \\ &= \sum_{s=0}^{L-2} \frac{1}{L-1} \frac{N_{\text{suc}, n_{w,-}>s}^{(w)}}{N_{\text{suc}}^{(w)}} + \zeta. \end{aligned}$$

To upper-bound $N_{\text{suc}, n_{w,-}>s}^{(w)}/N_{\text{suc}}^{(w)}$, whose trivial upper bound is 1, we use the fact that the number $N_{\text{suc}, n_{w,-}>s}^{(w)}$ of obtaining $n_{w,-} > s$ among the detected blocks can never be larger than the one $N_{\text{em}, n_{w,-}>s}^{(w)}$ among the emitted blocks. Since the probability of obtaining $n_{w,-} > s$ for any i^{th} block is upper-bounded by $\nu(L, s, C)$ from Eq. (13), we can imagine independent trials with probability $\nu(L, s, C)$. Therefore, again by using the Chernoff bound, we have that for any $\chi > 0$ and $\zeta > 0$

$$e_{\text{ph}}^{(w)} \leq \sum_{s=0}^{L-2} \frac{1}{L-1} \min \left\{ \frac{\nu(L, s, C) + \chi}{Q^{(w)}}, 1 \right\} + \zeta. \quad (14)$$

When we increase $N_{\text{suc}}^{(w)}$ for any fixed ζ and χ , the probability of violating Eq. (14) decreases exponentially. Therefore, in the limit of large $N_{\text{suc}}^{(w)}$, we can neglect these terms and finally obtain our main result in Eq. (9). Note that $Q^{(w)}$ is experimentally observed data. As will be shown in the next section, C is determined by the assumptions (A2) and (A3), namely, the parameters $\epsilon_1, \dots, \epsilon_{l_c}$ in Eq. (1) and the probabilities $p_{\text{vac},0}^{\text{L}}$ and $p_{\text{vac},1}^{\text{L}}$ in Eq. (2).

B. Derivation of X -basis measurement statistics using reference technique

Here, we derive the upper bound on $\Pr[x_t = -|\{x_k\}_{k \in \mathcal{P}_{i,m}}, j_{t-1}, \dots, j_{t-l_c}]$ in Eq. (12), regardless of $j_{t-1}, \dots, j_{t-l_c} \in \{0, 1\}^{l_c}$ that are the Z -basis measurement outcomes of systems $A_{t-1}, \dots, A_{t-l_c}$ in Eq. (7). The crucial point for its computation is that once $j_{t-1}, \dots, j_{t-l_c}$ are fixed, we find from Eq. (7) that the state of the systems $\mathbf{A}_{t-1} \mathbf{B}_{t-1}$ and the one of the systems $\mathbf{A}_{\geq t} \mathbf{B}_{\geq t}$ are decoupled, i.e., they are in the tensor product. The Z -basis measurement outcomes $j_{t-1}, \dots, j_{t-l_c}$ have an influence on determining the set of the t^{th} states $\{|\psi_{j_t|j_{t-1}}\rangle_{B_t}\}_{j_t}$, but the previous X -basis measurement outcomes $\{x_k\}_{k \in \mathcal{P}_{i,m}}$ have no influence on the state of the systems $\mathbf{A}_{\geq t} \mathbf{B}_{\geq t}$ thanks to the tensor product structure. Therefore, when conditioned on $j_{t-1}, \dots, j_{t-l_c}$, we only focus on the state of the systems $\mathbf{A}_{\geq t} \mathbf{B}_{\geq t}$ to calculate the target probability. From Eq. (7), conditioned on the outcomes $j_{t-1}, \dots, j_{t-l_c}$, the state of systems $\mathbf{A}_{\geq t} \mathbf{B}_{\geq t}$ is written as

$$|\Gamma_{j_{t-1}}^{\text{Act}}\rangle_{\mathbf{A}_{\geq t} \mathbf{B}_{\geq t}} := \frac{1}{\sqrt{2}} \sum_{j_t=0}^1 |j_t\rangle_{A_t} |\psi_{j_t|j_{t-1}}^{\text{Act}}\rangle_{\mathbf{A}_{\geq t+1} \mathbf{B}_{\geq t}} \quad (15)$$

with

$$\begin{aligned} |\psi_{j_t|j_{t-1}}^{\text{Act}}\rangle_{\mathbf{A}_{\geq t+1} \mathbf{B}_{\geq t}} &:= |\psi_{j_t|j_{t-1}}\rangle_{B_t} \otimes \\ &\quad \frac{1}{\sqrt{2^{N-t}}} \sum_{j_N} \dots \sum_{j_{t+1}} \bigotimes_{\zeta=t+1}^N |j_\zeta\rangle_{A_\zeta} |\psi_{j_\zeta|j_{\zeta-1}}\rangle_{B_\zeta}. \end{aligned} \quad (16)$$

As shown in [5], and also in Appendix B, Eq. (16) is rewritten as

$$\begin{aligned} |\psi_{j_t|j_{t-1}}^{\text{Act}}\rangle_{\mathbf{A}_{\geq t+1} \mathbf{B}_{\geq t}} &= |\psi_{j_t|j_{t-1}}\rangle_{B_t} \\ &\quad \left[a_{j_t, j_{t-1}} |\Phi_{j_{t-1}}\rangle_{\mathbf{A}_{\geq t+1} \mathbf{B}_{\geq t+1}} + b_{j_t, j_{t-1}} |\Phi_{j_t, j_{t-1}}^\perp\rangle_{\mathbf{A}_{\geq t+1} \mathbf{B}_{\geq t+1}} \right]. \end{aligned} \quad (17)$$

Here, $|\Phi_{j_{t-1}}\rangle$ and $|\Phi_{j_t, j_{t-1}}^\perp\rangle$ are normalized states that respectively does not contain the information of j_t and does contain its information. Note that the state $|\Phi_{j_{t-1}}\rangle$ represents a side-channel-free state, while the state $|\Phi_{j_t, j_{t-1}}^\perp\rangle$ represents the state of the side-channel since the information of j_t is propagated to the subsequence pulses. In our security proof, $|\Phi_{j_t, j_{t-1}}^\perp\rangle$ can be taken as any form in any-dimensional Hilbert space as long as it is orthogonal to $|\Phi_{j_{t-1}}\rangle$, and the characterization of $|\Phi_{j_t, j_{t-1}}^\perp\rangle$ is not required. The coefficient $a_{j_t, j_{t-1}}$ is positive and can be lower-bounded by using Eq. (1) as

$$a_{j_t=0, j_{t-1}} = 1, \quad a_{j_t=1, j_{t-1}} \geq \prod_{d=1}^{l_c} \sqrt{1 - \epsilon_d} \quad (18)$$

if $l_c \geq 1$ and $a_{j_t, j_{t-1}} = 1$ for both $j_t = 0, 1$ if $l_c = 0$ (see Appendix B for the detail).

Using Eq. (15), we have that the probability of our interest leads to

$$\begin{aligned} \Pr[x_t = - | \{x_k\}_{k \in \mathcal{P}_{i,m}}, j_{t-1}, \dots, j_{t-l_c}] \\ = \text{tr} \left[|-\rangle \langle -|_{A_t} |\Gamma_{j_{t-1}}^{\text{Act}}\rangle \langle \Gamma_{j_{t-1}}^{\text{Act}}|_{A_{\geq t} B_{\geq t}} \right]. \end{aligned} \quad (19)$$

To calculate Eq. (19), we introduce the reference states $\{|\phi_{j_t|j_{t-1}}^{\text{Ref}}\rangle_{A_{\geq t+1} B_{\geq t}}\}_{j_t}$ that are associated with the actual states $\{|\psi_{j_t|j_{t-1}}^{\text{Act}}\rangle_{A_{\geq t+1} B_{\geq t}}\}_{j_t}$. The reference states, which are close to the actual states prepared by the protocol, need to be chosen such that the following two conditions are satisfied. In its description, we use the notation

$$|\Gamma_{j_{t-1}}^{\text{Ref}}\rangle_{A_{\geq t} B_{\geq t}} := \frac{1}{\sqrt{2}} \sum_{j_t=0}^1 |j_t\rangle_{A_t} |\phi_{j_t|j_{t-1}}^{\text{Ref}}\rangle_{A_{\geq t+1} B_{\geq t}}. \quad (20)$$

(C1) For the reference state, the probability of obtaining the outcome of the minus when system A_t is measured in the X -basis is upper-bounded by constant $T > 0$, which is expressed as

$$\Pr[x_t = - | |\Gamma_{j_{t-1}}^{\text{Ref}}\rangle] \leq T. \quad (21)$$

(C2) The fidelity between $|\Gamma_{j_{t-1}}^{\text{Act}}\rangle$ and $|\Gamma_{j_{t-1}}^{\text{Ref}}\rangle$ is lower-bounded by constant $S > 0$, that is

$$\left| \langle \Gamma_{j_{t-1}}^{\text{Ref}} | \Gamma_{j_{t-1}}^{\text{Act}} \rangle \right| \geq S. \quad (22)$$

Once the reference states satisfy Eqs. (21) and (22), the upper bound on Eq. (19) can be obtained by using the function $g(x, y)$ [5] that relates the statistics of the actual and the reference states². Specifically, the X -basis measurement statistics of these two states are related as

$$\begin{aligned} \Pr[x_t = - | |\Gamma_{j_{t-1}}^{\text{Act}}\rangle] \\ \leq g \left(\Pr[x_t = - | |\Gamma_{j_{t-1}}^{\text{Ref}}\rangle], \left| \langle \Gamma_{j_{t-1}}^{\text{Ref}} | \Gamma_{j_{t-1}}^{\text{Act}} \rangle \right| \right), \end{aligned} \quad (23)$$

where $g(x, y) = x + (1-y^2)(1-2x) + 2y\sqrt{(1-y^2)x(1-x)}$ if $x \leq y^2$ and $g(x, y) = 1$ if $x > y^2$. A direct calculation reveals that if $x \leq y^2$,

$$g(x, y) \leq g(x^U, y^L) \quad (24)$$

holds, where U (L) indicates the upper (lower) bound. Then, combining Eqs. (21)-(24) gives

$$\Pr[x_t = - | |\Gamma_{j_{t-1}}^{\text{Act}}\rangle] \leq C = \begin{cases} g(T, S) & (\text{if } T \leq S^2) \\ 1 & (\text{if } T > S^2). \end{cases} \quad (25)$$

Hence, the remaining task for obtaining Eq. (12) is to derive the two bounds T and S , which are calculated below. In so doing, we take the reference state $|\phi_{j_t|j_{t-1}}^{\text{Ref}}\rangle_{A_{\geq t+1} B_{\geq t}}$ for $j_t \in \{0, 1\}$, which are associated with the actual state $|\psi_{j_t|j_{t-1}}^{\text{Act}}\rangle_{A_{\geq t+1} B_{\geq t}}$ in Eq. (17), such that it is the first term of $|\psi_{j_t|j_{t-1}}^{\text{Act}}\rangle_{A_{\geq t+1} B_{\geq t}}$:

$$|\phi_{j_t|j_{t-1}}^{\text{Ref}}\rangle_{A_{\geq t+1} B_{\geq t}} = |\psi_{j_t|j_{t-1}}^{\text{Act}}\rangle_{B_t} \otimes |\Phi_{j_{t-1}}\rangle_{A_{\geq t+1} B_{\geq t+1}}. \quad (26)$$

1. Calculation of T in Eq. (21)

We calculate the upper bound on $\Pr[x_t = - | |\Gamma_{j_{t-1}}^{\text{Ref}}\rangle]$. Let n_t be the number of photons contained in system B_t .

$$\begin{aligned} \Pr[x_t = - | |\Gamma_{j_{t-1}}^{\text{Ref}}\rangle] &= 1 - \Pr[x_t = + | |\Gamma_{j_{t-1}}^{\text{Ref}}\rangle] \\ &= 1 - \sum_{n=0}^{\infty} \Pr[n_t = n, x_t = + | |\Gamma_{j_{t-1}}^{\text{Ref}}\rangle] \\ &\leq 1 - \Pr[n_t = 0, x_t = + | |\Gamma_{j_{t-1}}^{\text{Ref}}\rangle]. \end{aligned}$$

By rewriting $|\Gamma_{j_{t-1}}^{\text{Ref}}\rangle$ using the X -basis states $|\pm\rangle_{A_t}$:

$$\begin{aligned} |\Gamma_{j_{t-1}}^{\text{Ref}}\rangle_{A_{\geq t} B_{\geq t}} &= |\Phi_{j_{t-1}}\rangle_{A_{\geq t+1} B_{\geq t+1}} \otimes \\ &\frac{|+\rangle_{A_t} \sum_{j_t} |\psi_{j_t|j_{t-1}}\rangle_{B_t} + |-\rangle_{A_t} \sum_{j_t} (-1)^{j_t} |\psi_{j_t|j_{t-1}}\rangle_{B_t}}{2}, \end{aligned} \quad (27)$$

we find that the statistics of n_t only depends on system A_t . Importantly, in obtaining Eq. (27), we used the fact that $|\Phi_{j_{t-1}}\rangle_{A_{\geq t+1} B_{\geq t+1}}$ is independent of j_t as stated in Sec. IV B. Then, combining Eq. (27) and the assumption (A3) in Sec. II C gives the lower-bound on $\Pr[n_t = 0, x_t = + | |\Gamma_{j_{t-1}}^{\text{Ref}}\rangle]$ as

$$\begin{aligned} \Pr[n_t = 0, x_t = + | |\Gamma_{j_{t-1}}^{\text{Ref}}\rangle] &= \left| \frac{\langle \text{vac} | \sum_{j_t} |\psi_{j_t|j_{t-1}}\rangle}{2} \right|^2 \\ &\geq \left[\sqrt{p_{\text{vac},0}^L} + \sqrt{p_{\text{vac},1}^L} \right]^2 / 4. \end{aligned}$$

In the inequality, we expand the orthonormal bases of $|\psi_0|j_{t-1}\rangle$ and $|\psi_1|j_{t-1}\rangle$ with the photon number states such that the coefficients of the vacuum states are positive. Therefore,

$$\Pr[x_t = - | |\Gamma_{j_{t-1}}^{\text{Ref}}\rangle] \leq 1 - \left(\sqrt{p_{\text{vac},0}^L} + \sqrt{p_{\text{vac},1}^L} \right)^2 / 4 = T.$$

² Note that the exact statement presented in [5] is that for any two normalized states $|A\rangle$ and $|R\rangle$ and any POVM (positive-operator-valued measure) $\{M, I - M\}$,

$$\text{tr}[|A\rangle\langle A|M] \leq g(\text{tr}[|R\rangle\langle R|M], |\langle A|R\rangle|).$$

2. Calculation of S in Eq. (22)

Next, we calculate the fidelity between $|\Gamma_{\mathbf{j}_{t-1}}^{\text{Act}}\rangle$ and $|\Gamma_{\mathbf{j}_{t-1}}^{\text{Ref}}\rangle$. We have that for $l_c \geq 1$

$$\begin{aligned} \left| \left\langle \Gamma_{\mathbf{j}_{t-1}}^{\text{Ref}} \middle| \Gamma_{\mathbf{j}_{t-1}}^{\text{Act}} \right\rangle \right| &= \frac{\left| \sum_{j_t} \left\langle \phi_{j_t \mid \mathbf{j}_{t-1}}^{\text{Ref}} \middle| \psi_{j_t \mid \mathbf{j}_{t-1}}^{\text{Act}} \right\rangle \right|}{2} \\ &= \frac{\left| \sum_{j_t} a_{j_t, \mathbf{j}_{t-1}} \right|}{2} \geq \frac{1 + \prod_{d=1}^{l_c} \sqrt{1 - \epsilon_d}}{2} = S. \end{aligned}$$

The first equality follows from Eqs. (15) and (20), the second equality comes from Eqs. (17) and (26), and the inequality follows from Eq. (18). If $l_c = 0$, $S = 1$ holds since $a_{j_t, \mathbf{j}_{t-1}} = 1$ for both $j_t = 0, 1$.

Data availability. No datasets were generated or analyzed during the current study.

Acknowledgements. This work is supported in part by the JSPS Grant-in-Aid for Scientific Research (C) No. 20K03779, (C) No. 21K03388, JST Moonshot R&D-MILLENNIA Program (grant number JPMJMS2061), and by JSPS KAKENHI Research (S) (Grants No: JP18H05237) CREST (Japan Science and Technology Agency) Grant No: JPMJCR1671.

Competing interests. The authors declare no competing interests.

Appendix A: Proof of Eq. (3)

Here, we prove Eq. (3). For this, once we obtain the following proposition, by substituting $|\psi\rangle = |\psi_{j_\zeta|j_{\zeta-1}, \dots, j_{k+1}, j_k=1, j_{k-1}, \dots, j_1}\rangle$, $|\phi\rangle = |\psi_{j_\zeta|j_{\zeta-1}, \dots, j_{k+1}, j_k=0, j_{k-1}, \dots, j_1}\rangle$ and the lower bounds in Eq. (2) to Eq. (A1), Eq. (3) can be obtained.

Proposition 1 For any state $|\psi\rangle$ and $|\phi\rangle$, a lower bound on the fidelity between these two states is given by

$$|\langle\psi|\phi\rangle| \geq \begin{cases} 2\sqrt{p_{\text{vac},\phi}p_{\text{vac},\psi}} - 1 & \text{if } 2\sqrt{p_{\text{vac},\phi}p_{\text{vac},\psi}} \geq 1 \\ 0 & \text{otherwise,} \end{cases} \quad (\text{A1})$$

where $p_{\text{vac},\phi} := \text{tr}[|\text{vac}\rangle\langle\text{vac}||\phi\rangle\langle\phi|]$.

(Proof) We expand $|\psi\rangle$ and $|\phi\rangle$ using the photon number states in all the optical modes, $|\text{vac}\rangle$ and $\{|n\rangle\}_{n \geq 1}$, as follows:

$$\begin{aligned} |\psi\rangle &= \sqrt{p_{\text{vac},\psi}}|\text{vac}\rangle + \sum_{n \geq 1} \beta_n |n\rangle, \\ |\phi\rangle &= \sqrt{p_{\text{vac},\phi}}|\text{vac}\rangle + \sum_{n \geq 1} \gamma_n |n\rangle. \end{aligned}$$

We here choose the global phase of $|\psi\rangle$ and $|\phi\rangle$ such that the coefficients of $|\text{vac}\rangle$ being positive, and $\beta_n \in \mathbb{C}$ and $\gamma_n \in \mathbb{C}$ are the coefficients for $n \geq 1$ of $|\psi\rangle$ and $|\phi\rangle$, respectively. By using this, $|\langle\psi|\phi\rangle|$ is written as

$$|\langle\psi|\phi\rangle| = \left| \sqrt{p_{\text{vac},\psi}}\sqrt{p_{\text{vac},\phi}} + e^{i\theta} \left| \sum_{n \geq 1} \beta_n^* \gamma_n \right| \right|, \quad (\text{A2})$$

where $\theta = \arg(\sum_{n \geq 1} \beta_n^* \gamma_n)$. We next derive the upper bound on $\left| \sum_{n \geq 1} \beta_n^* \gamma_n \right|$ by exploiting the triangle inequality and the Cauchy-Schwarz inequality:

$$\left| \sum_{n \geq 1} \beta_n^* \gamma_n \right| \leq \sum_{n \geq 1} |\beta_n| |\gamma_n| \leq \sqrt{\left(\sum_{n \geq 1} |\beta_n|^2 \right) \left(\sum_{n \geq 1} |\gamma_n|^2 \right)} = \sqrt{(1 - p_{\text{vac},\psi})(1 - p_{\text{vac},\phi})} =: \tau.$$

(i) If $2\sqrt{p_{\text{vac},\phi}p_{\text{vac},\psi}} \geq 1$, since $\sqrt{p_{\text{vac},\psi}}\sqrt{p_{\text{vac},\phi}} \geq \tau$ holds, Eq. (A2) is lower-bounded as follows:

$$\begin{aligned} |\langle\psi|\phi\rangle| &\geq \left| \sqrt{p_{\text{vac},\psi}}\sqrt{p_{\text{vac},\phi}} + e^{i\pi}\tau \right| \\ &= \sqrt{p_{\text{vac},\psi}}\sqrt{p_{\text{vac},\phi}} - \sqrt{(1 - p_{\text{vac},\psi})(1 - p_{\text{vac},\phi})} \\ &\geq \sqrt{p_{\text{vac},\psi}}\sqrt{p_{\text{vac},\phi}} - \sqrt{1 + p_{\text{vac},\psi}p_{\text{vac},\phi} - 2\sqrt{p_{\text{vac},\psi}}\sqrt{p_{\text{vac},\phi}}} \\ &= 2\sqrt{p_{\text{vac},\phi}p_{\text{vac},\psi}} - 1. \end{aligned}$$

The second inequality follows from the fact that $a + b \geq 2\sqrt{ab}$ holds for any $a, b \geq 0$.

(ii) If $2\sqrt{p_{\text{vac},\phi}p_{\text{vac},\psi}} < 1$, we only have the trivial lower bound:

$$|\langle\psi|\phi\rangle| \geq 0. \quad (\text{A3})$$

Appendix B: Proof of Eqs. (17) and (18)

In this appendix, we prove Eqs. (17) and (18). We start from Eq. (16):

$$|\psi_{j_t|j_{t-1}}^{\text{Act}}\rangle_{\mathbf{A}_{\geq t+1}\mathbf{B}_{\geq t}} = e^{i\theta_{j_t|j_{t-1}}} |\psi_{j_t|j_{t-1}}\rangle_{B_t} \left(\frac{1}{\sqrt{2^{N-t}}} \sum_{j_N} \cdots \sum_{j_{t+1}} \bigotimes_{\zeta=t+1}^N |j_\zeta\rangle_{A_\zeta} e^{i\theta_{j_\zeta|j_{\zeta-1}}} |\psi_{j_\zeta|j_{\zeta-1}, \dots, j_{t+1}, j_t, j_{t-1}}\rangle_{B_\zeta} \right). \quad (\text{B1})$$

Note that the phase $e^{i\theta_{j_\zeta|j_{\zeta-1}}}$ is added to the state $|\psi_{j_\zeta|j_{\zeta-1}, \dots, j_{t+1}, j_t, \mathbf{j}_{t-1}}\rangle_{B_\zeta}$. Since any states are equivalent up to a global phase, Eqs. (16) and (B1) are equal. The reason for adding the phase is to derive the lower bound on $a_{j_t, \mathbf{j}_{t-1}}$ for $j_t \in \{0, 1\}$, where the explicit form of $e^{i\theta_{j_\zeta|j_{\zeta-1}}}$ will be given in Eq. (B5).

To see how the information j_t is encoded to the state $|\psi_{j_t|j_{t-1}}^{\text{Act}}\rangle_{\mathbf{A}_{\geq t+1} \mathbf{B}_{\geq t}}$, we expand it using $|\Phi_{\mathbf{j}_{t-1}}\rangle_{\mathbf{A}_{\geq t+1} \mathbf{B}_{\geq t+1}}$ and $|\Phi_{j_t, \mathbf{j}_{t-1}}^\perp\rangle_{\mathbf{A}_{\geq t+1} \mathbf{B}_{\geq t+1}}$ to have

$$|\psi_{j_t|j_{t-1}}^{\text{Act}}\rangle_{\mathbf{A}_{\geq t+1} \mathbf{B}_{\geq t}} = e^{i\theta_{j_t|j_{t-1}}} |\psi_{j_t|j_{t-1}}\rangle_{B_t} \otimes \left(a_{j_t, \mathbf{j}_{t-1}} |\Phi_{\mathbf{j}_{t-1}}\rangle_{\mathbf{A}_{\geq t+1} \mathbf{B}_{\geq t+1}} + b_{j_t, \mathbf{j}_{t-1}} |\Phi_{j_t, \mathbf{j}_{t-1}}^\perp\rangle_{\mathbf{A}_{\geq t+1} \mathbf{B}_{\geq t+1}} \right), \quad (\text{B2})$$

where $|\Phi_{\mathbf{j}_{t-1}}\rangle_{\mathbf{A}_{\geq t+1} \mathbf{B}_{\geq t+1}}$ and $|\Phi_{j_t, \mathbf{j}_{t-1}}^\perp\rangle_{\mathbf{A}_{\geq t+1} \mathbf{B}_{\geq t+1}}$ denote some normalized states, and these are orthogonal each other. The subscripts in $a_{j_t, \mathbf{j}_{t-1}}$, $b_{j_t, \mathbf{j}_{t-1}}$, $|\Phi_{\mathbf{j}_{t-1}}\rangle_{\mathbf{A}_{\geq t+1} \mathbf{B}_{\geq t+1}}$, and $|\Phi_{j_t, \mathbf{j}_{t-1}}^\perp\rangle_{\mathbf{A}_{\geq t+1} \mathbf{B}_{\geq t+1}}$ indicate the dependency on the previous setting choices³. Importantly, $|\Phi_{\mathbf{j}_{t-1}}\rangle_{\mathbf{A}_{\geq t+1} \mathbf{B}_{\geq t+1}}$ does not depend on j_t but $|\Phi_{j_t, \mathbf{j}_{t-1}}^\perp\rangle_{\mathbf{A}_{\geq t+1} \mathbf{B}_{\geq t+1}}$ does. This means that $|\Phi_{j_t, \mathbf{j}_{t-1}}^\perp\rangle_{\mathbf{A}_{\geq t+1} \mathbf{B}_{\geq t+1}}$ represents the side-channel state of j_t . For $|\Phi_{\mathbf{j}_{t-1}}\rangle_{\mathbf{A}_{\geq t+1} \mathbf{B}_{\geq t+1}}$, we can take any state as long as it is independent of j_t . Here, we choose it as

$$\begin{aligned} |\Phi_{\mathbf{j}_{t-1}}\rangle_{\mathbf{A}_{\geq t+1} \mathbf{B}_{\geq t+1}} &= \frac{1}{\sqrt{2^{N-t}}} \left(\sum_{j_{t+l_c}} \cdots \sum_{j_{t+1}} \bigotimes_{\zeta=t+1}^{t+l_c} |j_\zeta\rangle_{A_\zeta} |\psi_{j_\zeta|j_{\zeta-1}, \dots, j_{t+1}, j_t=0, \mathbf{j}_{t-1}}\rangle_{B_\zeta} \right) \\ &\otimes \left(\sum_{j_N} \cdots \sum_{j_{t+l_c+1}} \bigotimes_{\zeta=t+l_c+1}^N e^{i\theta_{j_\zeta|j_{\zeta-1}}} |j_\zeta\rangle_{A_\zeta} |\psi_{j_\zeta|j_{\zeta-1}, \dots, j_{t+1}, j_t=0, \mathbf{j}_{t-1}}\rangle_{B_\zeta} \right) \end{aligned} \quad (\text{B3})$$

that corresponds to the $N-t$ systems of Eq. (B1) with j_t being fixed to be 0 and with omitting the phase from the state $\{|\psi_{j_\zeta|j_{\zeta-1}, \dots, j_{t+1}, j_t=0, \mathbf{j}_{t-1}}\rangle_{B_\zeta}\}_{\zeta=t+1}^{t+l_c}$. The reason for omitting the phase is to guarantee the positivity of $a_{j_t, \mathbf{j}_{t-1}}$ in Eq. (B2). The remaining task is to derive the lower bound on $a_{j_t, \mathbf{j}_{t-1}}$ for $j_t \in \{0, 1\}$ using the assumption (A2) in Sec. II C. Since $a_{j_t, \mathbf{j}_{t-1}}$ is the inner product between Eq. (B3) and the vector

$$\frac{1}{\sqrt{2^{N-t}}} \sum_{j_N} \cdots \sum_{j_{t+1}} \bigotimes_{\zeta=t+1}^N |j_\zeta\rangle_{A_\zeta} e^{i\theta_{j_\zeta|j_{\zeta-1}}} |\psi_{j_\zeta|j_{\zeta-1}, \dots, j_{t+1}, j_t, \mathbf{j}_{t-1}}\rangle_{B_\zeta},$$

which is the state of the $N-t$ systems shown in the parenthesis of Eq. (B1), we have

$$\begin{aligned} a_{j_t, \mathbf{j}_{t-1}} &= \frac{1}{2^{N-t}} \left(\sum_{j_{t+l_c}} \cdots \sum_{j_{t+1}} \prod_{\zeta=t+1}^{t+l_c} e^{i\theta_{j_\zeta|j_{\zeta-1}}} \langle \psi_{j_\zeta|j_{\zeta-1}, \dots, j_{t+1}, j_t=0, \mathbf{j}_{t-1}} | \psi_{j_\zeta|j_{\zeta-1}, \dots, j_{t+1}, j_t, \mathbf{j}_{t-1}} \rangle \right) \left(\sum_{j_N} \cdots \sum_{j_{t+l_c+1}} 1 \right) \\ &= \frac{1}{2^{l_c}} \sum_{j_{t+l_c}} \cdots \sum_{j_{t+1}} \prod_{\zeta=t+1}^{t+l_c} e^{i\theta_{j_\zeta|j_{\zeta-1}}} \langle \psi_{j_\zeta|j_{\zeta-1}, \dots, j_{t+1}, j_t=0, \mathbf{j}_{t-1}} | \psi_{j_\zeta|j_{\zeta-1}, \dots, j_{t+1}, j_t, \mathbf{j}_{t-1}} \rangle \\ &= \frac{1}{2^{l_c}} \sum_{j_{t+l_c}} \cdots \sum_{j_{t+1}} \prod_{\zeta=t+1}^{t+l_c} |\langle \psi_{j_\zeta|j_{\zeta-1}, \dots, j_{t+1}, j_t=0, \mathbf{j}_{t-1}} | \psi_{j_\zeta|j_{\zeta-1}, \dots, j_{t+1}, j_t, \mathbf{j}_{t-1}} \rangle|. \end{aligned} \quad (\text{B4})$$

In the second equality, we set the phases $e^{i\theta_{j_\zeta|j_{\zeta-1}}}$ for any ζ ($t+1 \leq \zeta \leq t+l_c$) and \mathbf{j}_N as

$$e^{i\theta_{j_\zeta|j_{\zeta-1}}} := \frac{|\langle \psi_{j_\zeta|j_{\zeta-1}, \dots, j_{t+1}, j_t=0, \mathbf{j}_{t-1}} | \psi_{j_\zeta|j_{\zeta-1}, \dots, j_{t+1}, j_t, \mathbf{j}_{t-1}} \rangle|}{\langle \psi_{j_\zeta|j_{\zeta-1}, \dots, j_{t+1}, j_t=0, \mathbf{j}_{t-1}} | \psi_{j_\zeta|j_{\zeta-1}, \dots, j_{t+1}, j_t, \mathbf{j}_{t-1}} \rangle}. \quad (\text{B5})$$

Since the only difference between both states in the inner product of Eq. (B4) is in the j_t^{th} index, we have

$$a_{j_t=0, \mathbf{j}_{t-1}} = 1.$$

³ Note that these subscripts are j_t, j_{t-1}, \dots, j_1 if $1 \leq t \leq l_c + 1$, and $j_t, j_{t-1}, \dots, j_{t-l_c}$ if $l_c + 2 \leq t$.

On the other hand, if $j_t = 1$, by applying Eq. (1) to Eq. (B4), we obtain

$$\begin{aligned} a_{j_t=1, j_{t-1}} &\geq \frac{1}{2^{l_c}} \sum_{j_{t+l_c}} \cdots \sum_{j_{t+1}} \prod_{\zeta=t+1}^{t+l_c} \sqrt{1 - \epsilon_{\zeta-t}} \\ &= \prod_{d=1}^{l_c} \sqrt{1 - \epsilon_d}. \end{aligned}$$

This ends the proof of Eqs. (17) and (18). \blacksquare

[1] H.-K. Lo, M. Curty, and K. Tamaki, *Nature Photonics* **8**, 595 (2014).
[2] K. Yoshino, M. Fujiwara, K. Nakata, T. Sumiya, T. Sasaki, M. Takeoka, M. Sasaki, A. Tajima, M. Koashi, and A. Tomita, *npj Quantum Information* **4**, 8 (2018).
[3] E. Diamanti, H.-K. Lo, B. Qi, and Z. Yuan, *npj Quantum Information* **2**, 16025 (2016).
[4] V. Zapatero, A. Navarrete, K. Tamaki, and M. Curty, arXiv:2105.11165v1 (2021).
[5] M. Pereira, G. Kato, A. Mizutani, M. Curty, and K. Tamaki, *Science Advances* **6**, eaaz4487 (2020).
[6] A. Mizutani, G. Kato, K. Azuma, M. Curty, R. Ikuta, T. Yamamoto, N. Imoto, H. K. Lo, and K. Tamaki, *npj Quantum Information* **5**, 8 (2019).
[7] T. Sasaki, Y. Yamamoto, and M. Koashi, *Nature* **509**, 475 (2014).
[8] A. Mizutani, N. Imoto, and K. Tamaki, *Phys. Rev. A* **92**, 060303 (2015).
[9] H.-L. Yin, Y. Fu, Y. Mao, and Z.-B. Chen, *Phys. Rev. A* **93**, 022330 (2016).
[10] Z. Zhang, X. Yuan, Z. Cao, and X. Ma, *New Journal of Physics* **19**, 033013 (2017).
[11] T. Sasaki and M. Koashi, *Quantum Science and Technology* **2**, 024006 (2017).
[12] Y. Hatakeyama, A. Mizutani, G. Kato, N. Imoto, and K. Tamaki, *Phys. Rev. A* **95**, 042301 (2017).

[13] L. Wang and S. Zhao, *Quantum Information Processing* **16**, 100 (2017).
[14] L. Liu, F.-Z. Guo, S.-J. Qin, and Q.-Y. Wen, *Scientific Reports* **7**, 42261 (2017).
[15] Z.-Q. Yin, S. Wang, W. Chen, Y.-G. Han, R. Wang, G.-C. Guo, and Z.-F. Han, *Nature Communications* **9**, 457 (2018).
[16] T. Matsuura, T. Sasaki, and M. Koashi, *Phys. Rev. A* **99**, 042303 (2019).
[17] H. Takesue, T. Sasaki, K. Tamaki, and M. Koashi, *Nature Photonics* **9**, 827 (2015).
[18] S. Wang, Z.-Q. Yin, W. Chen, D.-Y. He, X.-T. Song, H.-W. Li, L.-J. Zhang, Z. Zhou, G.-C. Guo, and Z.-F. Han, *Nature Photonics* **9**, 832 (2015).
[19] J.-Y. Guan, Z. Cao, Y. Liu, G.-L. Shen-Tu, J. S. Pelc, M. M. Fejer, C.-Z. Peng, X. Ma, Q. Zhang, and J.-W. Pan, *Phys. Rev. Lett.* **114**, 180502 (2015).
[20] Y.-H. Li, Y. Cao, H. Dai, J. Lin, Z. Zhang, W. Chen, Y. Xu, J.-Y. Guan, S.-K. Liao, J. Yin, et al., *Phys. Rev. A* **93**, 030302 (2016).
[21] F. Bouchard, A. Sit, K. Heshami, R. Fickler, and E. Karimi, *Phys. Rev. A* **98**, 010301 (2018).
[22] M. Koashi, *New Journal of Physics* **11**, 045018 (2009).
[23] M. Ben-Or, M. Horodecki, D. W. Leung, D. Mayes, and J. Oppenheim, *Second Theory of Cryptography Conf. TCC (Lecture Notes in Computer Science vol 3378)* (Berlin: Springer) pp 386-406 (2005).